Applied Microbiology and Biotechnology
https://doi.org/10.1007/s00253-019-10297-0

APPLIED GENETICS AND MOLECULAR BIOTECHNOLOGY

A pH-responsive genetic sensor for the dynamic regulation of D-xylonic acid accumulation in *Escherichia coli*

Angelo B. Bañares[1] · Kris Niño G. Valdehuesa[1] · Kristine Rose M. Ramos[1] · Grace M. Nisola[1] · Won-Keun Lee[2] · Wook-Jin Chung[1]

Received: 1 October 2019 / Revised: 28 November 2019 / Accepted: 3 December 2019

Abstract

The xylose oxidative pathway (XOP) is continuously gaining prominence as an alternative for the traditional pentose assimilative pathways in prokaryotes. It begins with the oxidation of D-xylose to D-xylonic acid, which is further converted to α-ketoglutarate or pyruvate + glycolaldehyde through a series of enzyme reactions. The persistent drawback of XOP is the accumulation of D-xylonic acid intermediate that causes culture media acidification. This study addresses this issue through the development of a novel pH-responsive synthetic genetic controller that uses a modified transmembrane transcription factor called CadCΔ. This genetic circuit was tested for its ability to detect extracellular pH and to control the buildup of D-xylonic acid in the culture media. Results showed that the pH-responsive genetic sensor confers dynamic regulation of D-xylonic acid accumulation, which adjusts with the perturbation of culture media pH. This is the first report demonstrating the use of a pH-responsive transmembrane transcription factor as a transducer in a synthetic genetic circuit that was designed for XOP. This may serve as a benchmark for the development of other genetic controllers for similar pathways that involve acidic intermediates.

Keywords Xylose oxidative pathway · D-xylonic acid · Dahms pathway · CadC · Transcription factor · Biosensor

Introduction

In recent years, there has been an increasing interest in the development of microbial cell factories using D-xylose as a substrate. D-xylose is advantageous over other sugars as it mainly comprises the pentose content (up to 35%) of lignocellulosic biomasses as promising renewable resources which do not compete with food crops (Gírio et al. 2010). Moreover, the unconventional D-xylose oxidative pathway (XOP) has been successfully employed as the main biosynthetic pathway for the production of many renewable and valuable compounds (Valdehuesa et al. 2018). Such biological platforms involved industrial microbial hosts like *Saccharomyces cerevisiae*, *Klebsiella pneumoniae*, *Pseudomonas putida*, and *Corynebacterium glutamicum* that were engineered either to grow on D-xylose through the XOP or to produce D-xylonic acid, glycolic acid, or ethylene glycol (Meijnen et al. 2009; Radek et al. 2014; Wang et al. 2016; Salusjärvi et al. 2017). Majority of successful XOP manipulations were performed in *Escherichia coli* for the production of ethylene glycol (Liu et al. 2013), glycolic acid (Cabulong et al. 2018a), 1,2,4-butanetriol (Valdehuesa et al. 2014), 1,4-butanediol (Liu and Lu 2015), and poly(lactate-*co*-glycolate) biopolymer (Choi et al. 2016). The aforementioned compounds are of industrial interest because of their widespread importance in various applications. For example, ethylene glycol serves as

Angelo B. Bañares and Kris Niño G. Valdehuesa contributed equally to this work.

Electronic supplementary material The online version of this article (https://doi.org/10.1007/s00253-019-10297-0) contains supplementary material, which is available to authorized users.

✉ Won-Keun Lee
wklee@mju.ac.kr

✉ Wook-Jin Chung
wjc0828@gmail.com

[1] Department of Energy Science and Technology (DEST), Energy and Environment Fusion Technology Center (E2FTC), Myongji University, Myongji-ro 116, Cheoin-gu, Yongin 17058, Gyeonggi-do, Republic of Korea

[2] Division of Bioscience and Bioinformatics, Myongji University, Myongji-ro 116, Cheoin-gu, Yongin 17058, Gyeonggi-do, Republic of Korea

Published online: 03 January 2020

an antifreeze agent and as a precursor for poly (ethylene terephthalate).

The XOP begins with the oxidation of D-xylose to D-xylonic acid by an NAD^+-dependent xylose dehydrogenase. This is followed by dehydration of D-xylonic acid into 2-keto-3-deoxy-D-pentonate (KDX) by a xylonate dehydratase. KDX may go through (1) the Weimberg route (Weimberg 1961), wherein it is dehydrated and then oxidized to form α-ketoglutarate or (2) Dahms route (Dahms 1974), wherein it undergoes aldol cleavage between carbon 3 and 4 to form pyruvate and glycolaldehyde. These two XOP routes have one persistent problem – the extracellular accumulation of D-xylonic acid (Bañares et al. 2019). Traditional metabolic engineering strategies have been implemented to address this issue, such as pathway optimization by identifying bottlenecks and selection of the best enzymes for the downstream conversions (Valdehuesa et al. 2015; Sun et al. 2016; Cabulong et al. 2017; Cabulong et al. 2018a), promoter modifications (Cabulong et al. 2017), and maintenance of redox homeostasis (Wang et al. 2018; Cabulong et al. 2018b). Synthetic biology tools have also been used for the improvement of XOP as exemplified by the development of an auto-inducible system using quorum sensing mechanism for the production of 1,4-butanediol in *E. coli* (Liu and Lu 2015). This was done to control the flux of D-xylose as a sole carbon source for 1,4-butanediol production and LB medium for cellular growth and maintenance. Recently, a D-xylonate-responsive promoter was employed to directly regulate the xylose dehydrogenase expression (Bañares et al. 2019). These strategies have, to a certain degree, minimized D-xylonic acid accumulation while improving the titer of a target compound.

Earlier works have shown that secretion of excess D-xylonic acid causes culture media acidification, which is detrimental to the cell growth and re-assimilation of the same metabolite (Liu et al. 2012; Valdehuesa et al. 2014). These changes in the extracellular pH are detected by *E. coli* through its several pH sensing systems. One of the extensively studied pH-responsive systems is the transmembrane one-component regulator called the CadC (Fig. 1). It is a membrane-integrated one-component bitopic protein with a periplasmic sensor domain and an intracellular winged helix-turn-helix DNA-binding domain (Jung et al. 2018). This transcriptional regulator is activated by low extracellular pH and lysine (Neely and Olson 1996). Its periplasmic domain directly senses the decrease in extracellular pH (less than 6.8) through a patch of acidic amino acids (D198, D200, E461, E468, and D471), which undergo protonation when exposed to low pH resulting in dimerization of the periplasmic domain, triggering receptor activation (Jung et al. 2018; Dell et al. 1994; Haneburger et al. 2011; Eichinger et al. 2011; Lindner and White 2014). However, the pH sensitivity of CadC can only be activated upon destabilization of its interaction with the lysine permease (LysP). The CadC complex with LysP is relieved in the presence of extracellular lysine at a concentration greater than 0.5 mM (Tetsch et al. 2008; Fritz et al. 2009). The signal from both stimuli then promotes the interaction between the DNA-binding domain and the *cadBA* promoter, which activates the expression of the lysine decarboxylase CadA and the lysine/cadaverine antiporter (CadB). CadA converts lysine to cadaverine, while CadB secretes cadaverine, which triggers feedback inhibition toward CadC (Watson et al. 1992; Takayama et al. 1994; Dell et al. 1994; Fritz et al. 2009; Haneburger et al. 2012). Its mode of signal transduction is rare as the full-length

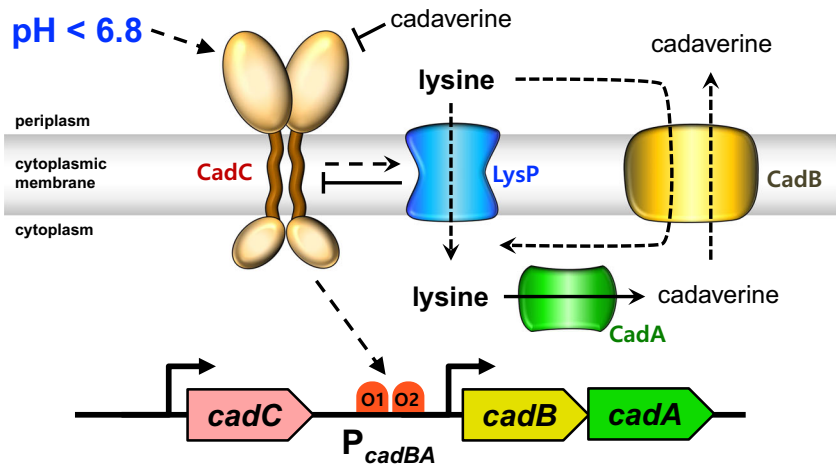

Fig. 1 Mechanism for the one-component bacterial transmembrane signaling system CadC for the transcriptional activation of lysine decarboxylase (CadA) and lysine/cadaverine antiporter triggered by extracellular acidification and lysine accumulation. In the absence of lysine and neutral pH, the lysine transporter LysP binds to the transmembrane domain of CadC and deactivates transcription. The accumulation of lysine causes LysP to dissociate from CadC upon importing lysine into the cell. In conjunction with LysP dissociation, the extracellular lysine also causes acidification which leads to expression of CadB and CadA. The former converts lysine to cadaverine while the latter secretes cadaverine. Finally, cadaverine accumulates and acts as a feedback inhibitor to CadC

membrane-integrated receptor binds to *cadBA* promoter without proteolytic cleavage (Fritz et al. 2009; Haas et al. 2015).

CadC variants that bypass the requirement for the lysine-mediated stimuli and rely solely on pH sensing have been described previously (Neely et al. 1994; Tetsch et al. 2008). One mutant of particular interest is the CadCΔ in which the heptapeptide chain at position 159 to 165 has been removed (Tetsch et al. 2008). This deletion rendered the CadCΔ independent from lysine. Noting that D-xylonic acid buildup causes media acidification and that CadCΔ is exclusively pH-sensitive, a pH-responsive genetic sensor for the regulation of D-xylonic acid accumulation is proposed in this study. Reporter gene assays were initially performed to verify the pH-responsive activity of CadCΔ in a culture media that was acidified using an inorganic acid. The genetic sensor was then tested in *E. coli* BL21 strain that purposely accumulates D-xylonic acid to confirm the role of CadCΔ in mediating the regulation of xylose dehydrogenase and xylonolactonase expression encoded by *xdh* and *xylC*, respectively. Finally, the pH-responsive genetic sensor was integrated into *E. coli* W3110 strain that utilizes D-xylose through the Dahms route of the XOP to demonstrate its ability to control the buildup of D-xylonic acid. Fed-batch experiments were also performed to show the dynamic response of the genetic sensor.

Materials and method

DNA manipulations

The plasmids and strains used in this study are listed in Table 1. Standard techniques were used in all genetic manipulation experiments (Green and Sambrook 2012), while the Gibson assembly technique was used for the construction of recombinant plasmids (Gibson et al. 2009). All PCR reactions were carried out using Phusion High-Fidelity DNA Polymerase using appropriate oligonucleotides (Table S1). Plasmid transformation was performed using the one-step transformation and storage solution protocol (Chung et al. 1989). The *sf*GFP was cloned from *sf*GFP-pBAD, which was generously provided by Michael Davidson and Geoffrey Waldo (Addgene

Table 1 Plasmids and strains names used in this study

Plasmids	Relative characteristics	Reference
pACM4	pACYC-Duet derivative; with ePathBrick feature; P_{T7}; Cm^r	(Xu et al. 2012)
pRSET-A	pUC *ori*, P_{T7}, Amp^R	Invitrogen
pRT7	pRSET-A carrying *sfGFP* under T7 promoter	This work
pRCadCΔ	pRSET-A carrying *sfGFP* under *cadBA* promoter; *cadC*Δ under T7 promoter	This work
pRBC	pRSET-A carrying codon-optimized *xylB* and *xylC* from *C. crescentus* under T7 promoter	This work
pRBCPH	pRSET-A carrying codon-optimized *xylB* and *xylC* from *C. crescentus* under T7 promoter, *lacI* under *cadBA* promoter, and *cadC*Δ under *lacIq* promoter	This work
pAB	pACM4 without *lacI* carrying *yjgB* from *E.coli* under *lacIq* promoter	This work
Strains		
E. coli DH5α	F^- *endA1 glnV44 thi-1 recA1 relA1 gyrA96 deoR nupG purB20* φ80d*lacZ*ΔM15 Δ(*lacZYA-argF*)U169, hsdR17($r_K^- m_K^+$), λ^-	Enzynomics
BL21(DE3)	F^- *ompT hsdSB*($r_B^- m_B^-$) *gal dcm* (DE3)	Invitrogen
BL21(DE3) Δ*xylAB*	BL21 (DE3) with deletion in *xylAB* genes	This work
E. coli W3110 (DE3) Δ*xylAB*	F^-mcrA mcrB IN(rrnD$^-$rrnE)1λ^-(DE3); ATCC No.27325; with *xylAB* deletion	(Liu et al. 2012)
E. coli W3110 Δ*xylAB*Δ*yjgB*Δ*aldA*	F^-mcrA mcrB IN(rrnD$^-$rrnE)1λ^-(DE3); ATCC 27325; with deletion in *xylA*, *xylB*, *yjgB* and *aldA* genes	(Cabulong et al. 2017)
BLC	BL21(DE) pRSET-A	This work
BLT7	BL21(DE) pRT7	This work
BLPH	BL21(DE) pRCadCΔ	This work
BLXA	BL21(DE3) Δ*xylAB* pRBC	This work
BLXAPH	BL21(DE3) Δ*xylAB* pRBCPH	This work
EWXA	*E. coli* W3110 (DE3) pRBC	This work
EWXAPH	*E. coli* W3110 (DE3) pRBCPH	This work
EWEG	*E. coli* W3110 Δ*xylAB*Δ*yjgB*Δ*aldA* pRBC pAB	This work
EWEGPH	*E. coli* W3110 Δ*xylAB*Δ*yjgB*Δ*aldA* pRBCPH pAB	This work

plasmid #54519) (Pédelacq et al. 2006). The *cadBA* promoter, the *yjgB* gene, and the DNA fragments used to construct the *cadC* derivative, CadCΔ (Table S2), were amplified from the genome of *E. coli* W3110. The *xdh* gene was cloned from pX (Cabulong et al. 2018a), while the *xylC* gene was synthesized by Macrogen, Korea. The *rrnB* terminator and the *lacq* promoter were both amplified from the vector pTrcHis2A, while the T7 terminator was derived from pRSET-A plasmid. The full details of the cloning experiments were discussed in SI File 1. The sequence fidelity of all the constructed plasmids was confirmed by DNA sequencing.

Culture conditions

Propagation and maintenance of recombinant plasmids were done using *E. coli* DH5α grown on LB broth or agar supplemented with appropriate antibiotics (50 μg mL^{-1} kanamycin or 100 μg mL^{-1} ampicillin). Modified M9 (MM9) medium containing 33.7 mM Na_2HPO_4, 22.0 mM KH_2PO_4, 8.55 mM NaCl, 9.35 mM NH_4Cl, 1.0 mM $MgSO_4$, 0.5 g L^{-1} yeast extract, and 1.0 g L^{-1} peptone was used throughout the study. For the fluorescence analysis, MM9-1 media was used which consists of the MM9 media and 2.5 g L^{-1} D-glucose. For the fermentation experiments, MM9-2 media was used which consists of the MM9 media with the addition of 2 g L^{-1} casamino acid, 1.0 mM thiamine HCl, 0.1 mM $CaCl_2$, 0.4% glycerol (*v*/v), and 4 g L^{-1} D-xylose. The fed-batch experiments also used MM9-2 media, while the appropriate volume of feed added every 36 h contained concentrated MM9-2 media sufficient to compensate for the culture volume loss due to sampling. All batch (shake flask) and fed-batch fermentation runs were agitated at 200 rpm and incubated at 37 °C.

Fluorescence analysis

One mL aliquot of an overnight culture of the constructed *E. coli* strains in LB broth was washed with sterile MM9 media and then inoculated in MM9-1 media at pH 7.0. Upon reaching an optical density of 0.6 units (OD_{600nm}), expression of *sf*GFP was induced by lowering the media pH to 5.8 using 2 M sulfuric acid, while the control group was maintained at pH 7.0. The media pH was monitored throughout the experiment using Orion 4 Star benchtop pH meter with Orion 8102BN pH probe (Thermo Scientific, Korea). The bacterial cells were collected by centrifugation at 13,000 rpm for 2 min and resuspended in sterile deionized water. The fluorescence was then measured using FluoroMate FS-2 fluorescence spectrometer (Scinco, Korea) using the following parameters for *sf*GFP: 485 nm excitation, 507 nm emission.

Biomass and metabolite quantification

The dry cell weight (DCW) and metabolite concentrations were quantified using the same methods and conditions that were described previously (Liu et al. 2013). Briefly, the standard curve of DCW correlated to OD_{600nm} was 0.32 g L^{-1} DCW. On the other hand, the substrate and metabolite concentrations were quantified using HPLC equipped with a Bio-Rad Aminex HPX-87H column maintained at 55 °C. The eluent used was 5 mM H_2SO_4 at a constant flow rate of 0.4 mL min^{-1}, and peaks were detected using Waters 2414 refractive index detector.

Enzyme activity assay

The xylose dehydrogenase activity was measured from crude cell extracts according to the method reported previously (Berghäll et al. 2007; Liu et al. 2012). The cells were collected from the samples by centrifugation, washed with Tris HCl (50 mM, pH 8.0), and then resuspended in the same buffer. Cell lysis was done by incubation with 1 mg mL^{-1} of lysozyme for 30 min followed by sonication. The cell debris was removed by centrifugation, and the protein concentration of the crude lysate was determined using Bradford assay (Bradford 1976). The assay mixture contains Tris HCl (50 mM, pH 8.0), NAD^+ (100 mM), and an appropriate amount of crude lysate. The mixture was pre-incubated at 37 °C for 30 min; then the reaction was initiated by addition of 10 mM D-xylose. The generation of NADH was monitored 340 nm using 8453 Agilent UV-VIS spectrophotometer. One unit of D-xylose dehydrogenase activity is defined as the amount of enzyme that converted 1 μmol D-xylose to D-xylonic acid per minute, and the specific activity was calculated as enzyme activity per mg protein.

Gene accession numbers

The following are the gene accession numbers (Gene ID) of the genes cloned in this work: *cadC* (948653), codon-optimized *xylB* or simply referred as *xdh* (MF872191), codon-optimized *xylC* (7329903), *lacI* (945007), and *yjgB* (also known as *ahr*, 948,802).

Results

Construction of lysine-independent pH-responsive genetic sensor

A lysine-independent variant of CadC (Protein ID: KYO73866), named CadCΔ, was constructed based on earlier work (Tetsch et al. 2008). CadCΔ carries a deletion of

seven amino acid residues in its transmembrane helix at 159th–165th positions, which contain a cluster of aromatic amino acids, "FWVWFFF." This modification converted CadCΔ into a lysine-independent transcription factor since the aforementioned polypeptide is essential for LysP binding (Fig. 2A). Regarding the role of cadaverine, there is no evidence that feedback inhibition was still true for this variant (Tetsch et al. 2008), and this was not explored further as it is beyond the scope of this study.

The CadCΔ was then integrated into a simple AND gate (Boolean logic) synthetic genetic circuit wherein two ON input signals are required to generate an output signal (Fig. 2B). Input 1 is a constant ON signal since CadCΔ is constitutively expressed, while input 2 is dependent on the extracellular pH and is ON below its threshold value of 6.8. The expected output is the expression of the green fluorescence protein *sf*GFP, which is placed under the control of *cadBA* promoter that is recognized by CadCΔ.

The prototype synthetic genetic circuit was then introduced and tested in *E. coli* BL21 (Fig. 2C). Results reveal a fivefold increase of fluorescence signal after 12 h incubation at pH 5.8. This indicates that the pH genetic sensor effectively responds to the decrease in pH. Meanwhile, the slight increase of *sf*GFP expression at pH 7.0 after 12 h incubation may be attributed to the slight decrease in pH which was triggered by the accumulation of trace amounts of acetate from D-glucose. To avoid this, glycerol was chosen as the supplementing carbon source in the subsequent experiments. It is interesting to note that the acidification of the culture media can negatively affect the signal brightness of *sf*GFP due to its pH sensitivity (Roberts et al. 2016). This was observed when *sf*GFP was expressed using IPTG wherein the fluorescence signal (brightness) decreased by 36% at pH 5.8 compared to pH 7.0 (Fig. S2). Hence, the *sf*GFP signal intensity resulting from the CadCΔ transcription activation (Fig. 2C) may not be representative of the actual activation strength of CadCΔ at low pH; i.e., more *sf*GFP proteins may be present despite its lower apparent/quantified signal intensity.

pH genetic sensor response to D-xylonic acid accumulation in vivo

The constructed pH genetic sensor employing CadCΔ was then tested in *E. coli* BL21 which is incapable of assimilating D-xylonic acid (Valdehuesa et al. 2018). The premise is that D-xylonic acid accumulation will cause a drop in pH which cascades into a feedback signal that will block the expression of Xdh and XylC, thus preventing further D-xylonic acid accumulation (Fig. 3A). The resulting strain, BLXAPH, carries the complete synthetic genetic circuit that consists of the following parts: (1) a constitutively expressed CadCΔ, (2) the repressor protein LacI that is expressed under the control of *cadBA* promoter, and (3) the polycistronic expression of Xdh and XylC under a LacI-repressible promoter. As a control strain, BLXA was also constructed to constitutively express Xdh and XylC through the plasmid pRBC (Table 1 and Fig. S1).

BLXA and BLXAPH were cultivated in shake flasks for 72 h to monitor cell growth, medium pH, substrate consumption, and metabolite levels (Fig. 3B–F). Without the pH genetic sensor, BLXA completely consumed D-xylose and accumulated up to 3.80 g L^{-1} D-xylonic acid (Fig. 3B and C). The pH after 12 h was 5.7, while the final pH after 72 h was 5.6 (Fig. 3D). This has negatively affected the growth of BLXA which only reached a maximum DCW of 1.0 g L^{-1} (Fig. 3E). Meanwhile, BLXAPH behaved differently as the final pH of the culture medium after 72 h was 6.1 (pH 6.4 after 12 h) and the final D-xylonic acid concentration was at 3.2 g L^{-1}. This was due to the arrested D-xylose consumption which was observed after 12 h of cultivation. Interestingly, BLXAPH displayed better growth which may be due to the less stressful environment brought by the marginal decrease of extracellular pH (Fig. 3D and E). Overall, the results demonstrate that the pH genetic sensor effectively responded to the extracellular acidification. The presence of excess D-xylonic acid actively caused culture medium acidification (pH < 6.8) which then stimulated the CadCΔ to activate the expression

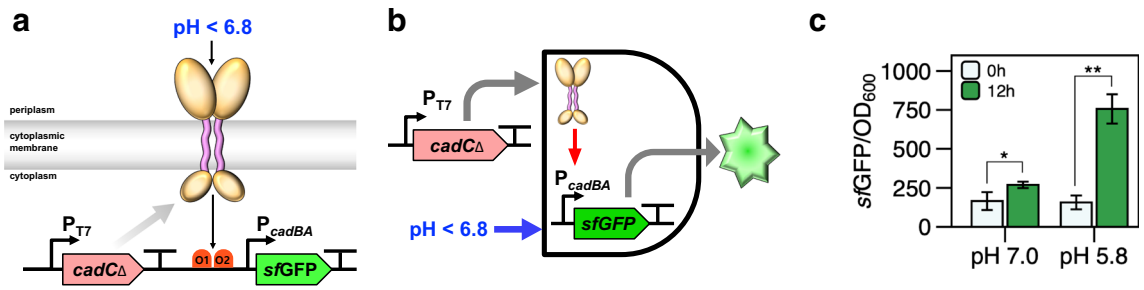

Fig. 2 Overview of mechanism for CadCΔ and its use in sensing low pH to express green fluorescent protein *sf*GFP in strain BLPH (*E. coli* BL21 pRCadCΔ). **A** Mechanism for the lysine-independent CadCΔ to detect low pH and trigger expression of *sf*GFP. **B** An AND gate Boolean logic diagram for the reporter gene assay using CadCΔ. **C** Reporter gene assay results for BLPH. The cells were pre-cultured at pH 7.0 for 12 h in MM9-1 media. To trigger CadCΔ-mediated *sf*GFP expression, the pH was adjusted to 5.8 using 2 M H_2SO_4. [$^*p < 0.05$; $^{**}p < 0.001$; Student T-test was used with $n \geq 3$]. Note: the constitutive expression for CadCΔ was mediated by the high basal/leaky activity of the T7 promoter in the absence of its cognate repressor, LacI

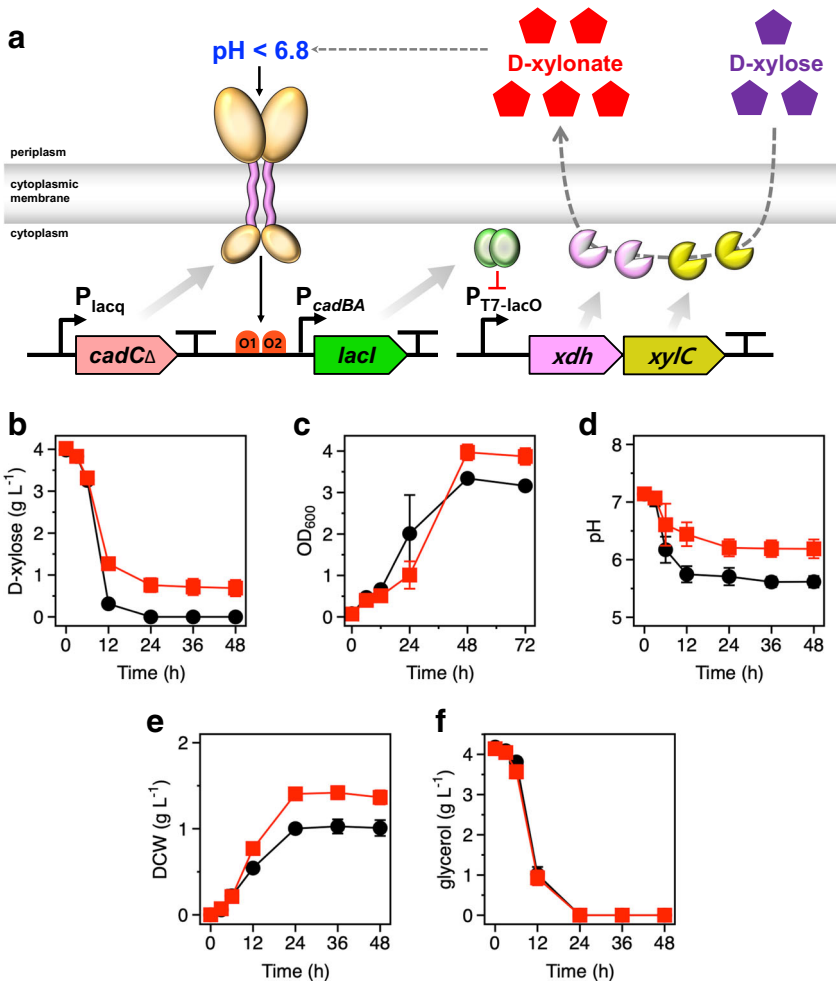

Fig. 3 Implementation of sensing and control of D-xylonic acid accumulation in *E. coli* BL21 strains BLXA and BLXAPH. **A** Schematic diagram of CadCΔ for controlling D-xylonic acid accumulation. **B** D-xylose consumption, **C** D-xylonic acid accumulation, **D** extracellular pH, **E** biomass concentration; *DCW* dry cell weight, and **F** glycerol consumption. BLXA carries constitutive expression of *xylC* and *xdh*; BLXAPH carries the sensor genetic circuit which regulates the expression of *xylC* and *xdh*. MM9-2 was used as the culture media. At least two independent trials were performed for both strains

of the LacI repressor. Consequently, the production of LacI effectively blocked Xdh and XylC expressions which prevented further D-xylonic acid accumulation. This observation validated the premise stated above.

pH genetic sensor for the Dahms pathway

The pH genetic sensor was then integrated into *E. coli* W3110 strain that is capable of assimilating D-xylonic acid through the Dahms Pathway (Valdehuesa et al. 2018). The mechanics in the EWXAPH strain is similar to BLXAPH with the added capability to re-assimilate any excess D-xylonic acid for growth and production of ethylene glycol or glycolic acid (Fig. 4). Xdh and XylC are initially expressed for the conversion of D-xylose to D-xylonic acid. Eventually, D-xylonic acid accumulates which triggers two events: (1) acidification of the culture media that leads to the depletion of enzymes that produces D-xylonic acid (Fig. 4A) and (2) the native activation of the expression of downstream enzymes for D-xylonic acid catabolism (Fig. 4B). The synergy of these two events is expected to result in the consumption of D-xylonic acid and pH neutralization of the culture media. As a control, EWXA was also constructed which constitutively expresses Xdh and XylC through the plasmid pRBC (Table 1 and Fig. S1).

EWXA and EXAPH were cultivated in shake flasks for 72 h to monitor the cell growth, Xdh activity, medium pH, as well as the levels of substrates, metabolites, and products (Fig. 5). For EWXA, D-xylose and glycerol were completely consumed after 24 h (Fig. 5A and B). The rapid conversion of D-xylose resulted in the accumulation of 3.5 g L^{-1} D-xylonic acid after 12 h (Fig. 5C) which caused severe media acidification at pH 5.4 (Fig. 5D). Similar to BLXA, EWXA also reached 1.0 g L^{-1} DCW after 24 h which coincided with the time point for substrate depletion (Fig. 5E). However, biomass concentration was slightly higher, which can be attributed to the D-xylonic acid re-assimilation phase after 24 h of cultivation. This is also the time point when ethylene glycol and glycolic acid are produced (Fig. 5F and G). Interestingly, the transient accumulation of 0.81 g L^{-1} glycolic acid after 36 h was not strong enough to affect the media pH since D-xylonic acid accumulation already caused severe media acidification.

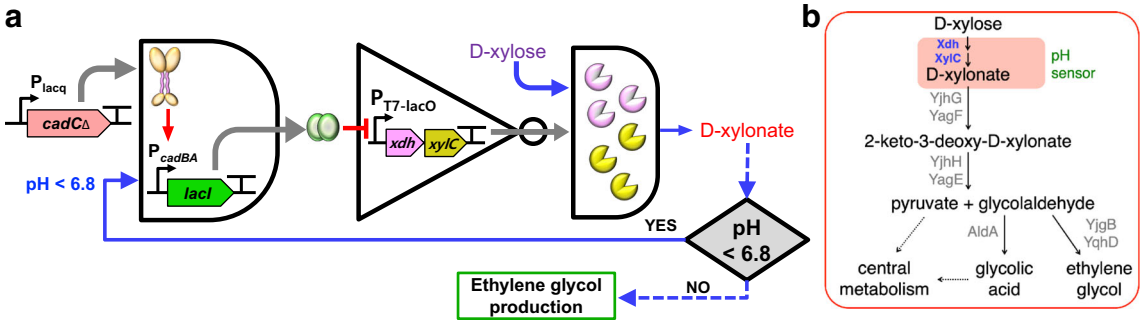

Fig. 4 The use of CadCΔ pH genetic sensor for ethylene glycol production in *E. coli* W3110. **A** An AND-NOT-AND Boolean logic diagram of the pH sensor for the control of D-xylonic acid accumulation during ethylene glycol production from D-xylose. **B** Metabolic pathway for ethylene glycol production in *E. coli* through the Dahms pathway with and integrated pH sensor

On the other hand, EWXAPH has a slightly different D-xylose consumption profile compared to EWXA. After 6 h, 0.6 g L^{-1} D-xylose was consumed, and the accumulation of 0.5 g L^{-1} D-xylonic acid was observed (Fig. 5C). This concentration of D-xylonic acid already caused a significant drop in the extracellular pH which plunged below the 6.8 threshold for CadCΔ activation. At this juncture, the pH genetic circuit is actively blocking further expression of Xdh and XylC as evidenced by the decrease in Xdh activity within 12 h (Fig. 5H). This resulted in a slower D-xylose conversion at only 2.0 g L^{-1} after 12 h (Fig. 5A) and the secretion of 2.0 g L^{-1} D-xylonic acid (Fig. 5C). Complete consumption of D-xylose was also observed after 24 h, which is the same point when the D-xylonic acid concentration peaked at 2.2 g L^{-1} (Fig. 5C) and the extracellular pH was lowest at 6.2 (Fig. 5D). Meanwhile, the biomass concentration of EWXAPH was significantly higher by 40% compared to EWXA (Fig. 5E). Ethylene glycol production was slightly improved, whereas glycolic acid accumulation was lower compared to EWXA (Fig. 5F and G). Interestingly, the extracellular pH reverted to near-neutral conditions during the re-assimilation of the secreted D-xylonic acid (at 24 to 36 h). Xdh activity also showed recovery during this period (Fig. 5H) which indicates that the synthetic genetic circuit is capable of switching back to its original state, thus, demonstrating great potential for dynamic regulation.

pH-dependent dynamic regulation of D-xylonic acid accumulation

To demonstrate the dynamic regulation of D-xylonic acid accumulation through the pH genetic sensor, the strain EWXAPH was tested in fed-batch conditions

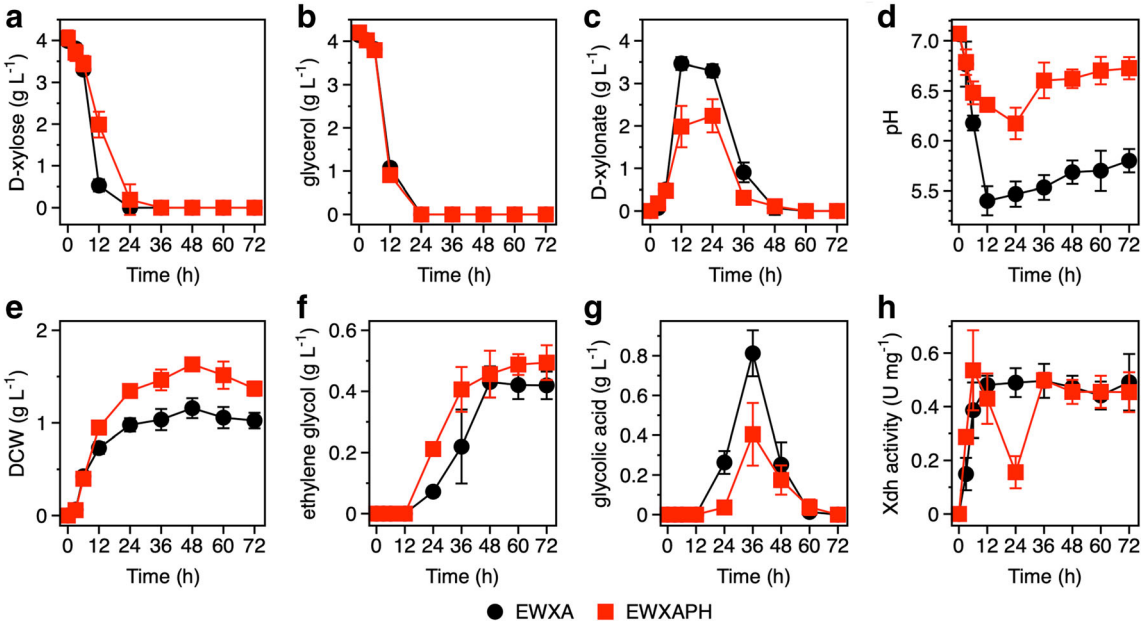

Fig. 5 Substrates, biomass, metabolites, products, pH, and enzyme activity measurements for *E. coli* W3110 strains EWXA and EWXAPH during conversion of D-xylose to ethylene glycol. **A** D-xylose consumption, **B** glycerol consumption, **C** D-xylonic acid concentration, **D** extracellular pH, **E** biomass concentration; *DCW* dry cell weight, **F** ethylene glycol concentration, **G** glycolic acid concentration, **D** xylose dehydrogenase, Xdh activity. EWXA carries constitutive expression of *xylC* and *xdh*; EWXAPH carries the sensor genetic circuit which regulates the expression of *xylC* and *xdh*. MM9-2 was used as the culture media. At least two independent trials were performed for both strains

without any external pH controller (i.e., maintaining media pH by addition of inorganic acid or base was omitted). The EWXA strain was also used as the control. Initial test cultures using 24 h feeding intervals were performed but were unsuccessful since the response lead time for the pH genetic sensor did not match the time required to achieve extracellular pH homeostasis, which is dependent on the D-xylonic acid re-assimilation (Fig. S3). Based on the batch cultures of EWXAPH (Fig. 5), a minimum of 36 h is required to complete one cycle. Hence, 36 h was used as a standard interval for the fed-batch experiments.

Results showed that the control strain EWXA has the same substrate consumption profiles throughout the three cycles (Fig. 6A). The biomass accumulation increased during the first cycle and remained at 2.2 g L^{-1} until the end of the third cycle. Additionally, extracellular pH drastically dropped to 5.2 within the first 12 h of cultivation (Fig. 6B), the same period when the concentration of D-xylonic acid was highest at ~3.8 g L^{-1} (Fig. 6C). Since EWXA does not carry the pH genetic sensor, the Xdh activity remained constant at ~0.6 U mg^{-1} throughout the experiment (Fig. 6B), which led to the accumulation of D-xylonic acid at > 3.0 g L^{-1} after every feeding cycle. The pH was also not able to revert to its neutral state after the complete re-assimilation of D-xylonic acid at 36 h (and at the end of the experiment), a similar behavior observed in the batch experiments for EWXA (Fig. 5C and D). Furthermore, the titer for ethylene glycol did not improve after 120 h compared to the batch culture (Fig. 5F and Fig. 6C). Overall, the lack of pH genetic sensor in EWXA caused the D-xylonic acid to accumulate, which led to severe media acidification. This may have triggered the expression of pathways or enzymes involved in coping with acid-induced cellular stress and may have also negatively affected the expression or activity of downstream enzymes for ethylene glycol production.

The performance of EWXAPH was significantly better than EWXA (Fig. 7). The substrate consumption profile was consistent at every cycle, and the biomass concentration was 23% higher (Fig. 7A). The extracellular pH dropped marginally to ~6.2 (Fig. 7B), which coincided with the highest D-xylonic acid concentration for each cycle at 12, 48, and 84 h (Fig. 7C). The pH genetic sensor appears to regulate Xdh and XylC expressions as evidenced by the rise and fall of Xdh activity which also occurred simultaneously with the extracellular pH oscillation (Fig. 7B). This demonstrates the ability of the pH genetic sensor to dynamically regulate D-xylonic acid accumulation via the pH-sensitive CadCΔ. The EWXAPH also showed enhanced ethylene glycol production at 2.3 g L^{-1} which is 170% higher compared to EWXA(Fig. 7C).

Discussion

Currently, there are a limited number of reports describing synthetic genetic circuits that integrated pH-responsive genetic parts. For example, the YGP1 promoter from yeast was engineered to improve its low pH sensitivity and then was used as a benchmark to convert the unrelated CCW14 promoter to be pH-sensitive for lactic acid production at low pH conditions (Rajkumar et al. 2016). The pH-responsive promoter P_{asr} from *E. coli* was used in the construction of complex genetic circuits designed to produce either an ON or OFF signal depending on the temperature and external pH (Hoynes-OConnor et al. 2017). The same pH-responsive promoter was employed in developing a pH-mediated kill switch for an effective bacterial containment system in *E. coli* (Stirling et al.

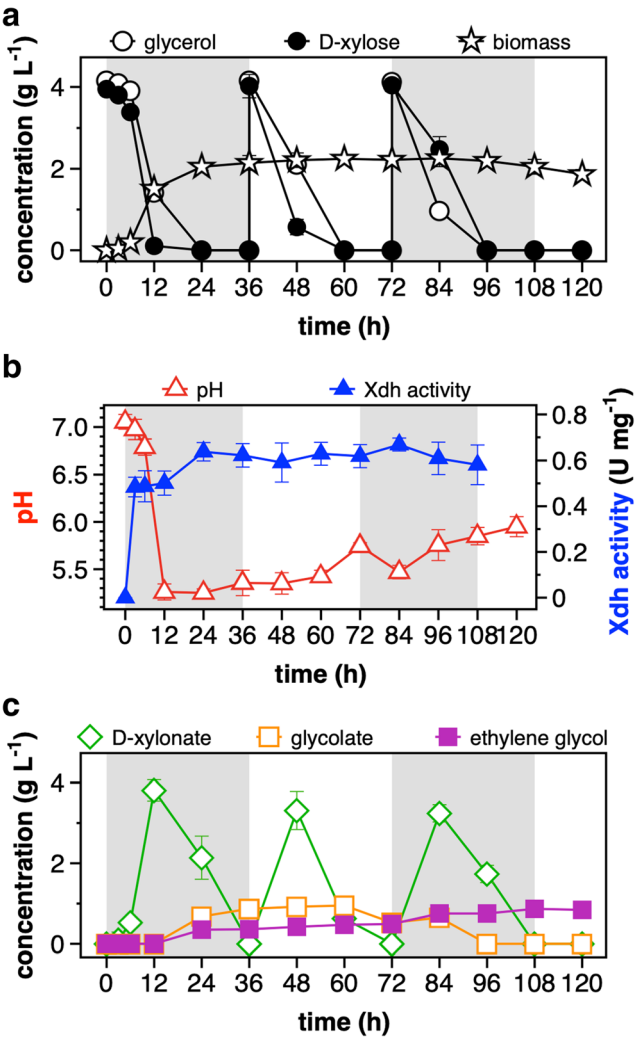

Fig. 6 Fed-batch cycles for EWXA. **A** Substrate concentration and biomass accumulation, **B** pH and Xdh activity measurements, and **C** D-xylonate, glycolate, and ethylene glycol concentrations. Alternate shading indicates different cycle times with 36 h intervals. At least two independent trials were performed for both strains

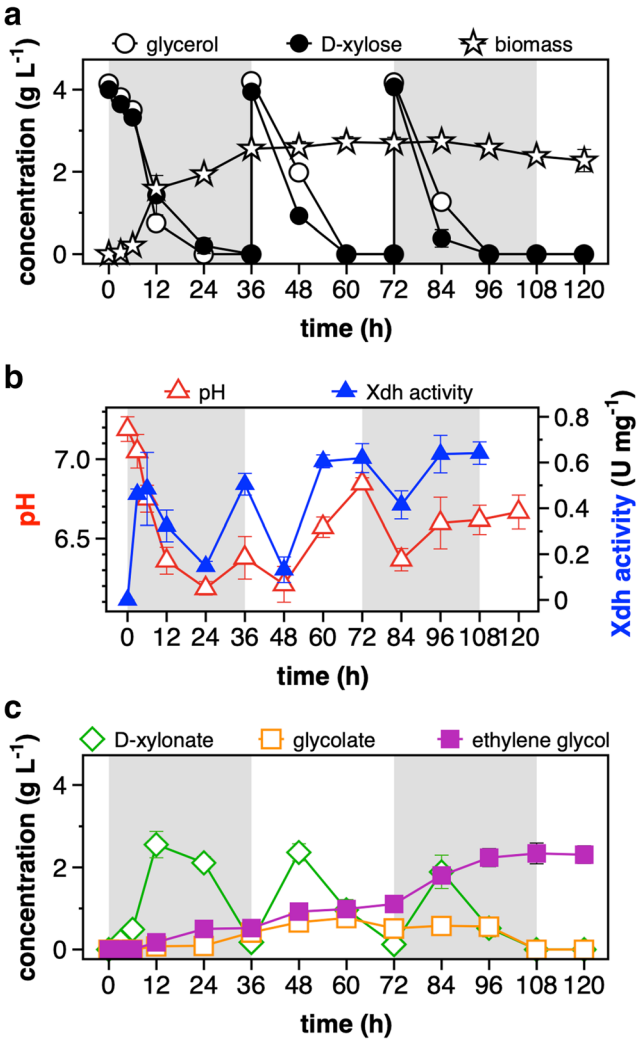

Fig. 7 Fed-batch cycles for EWXAPH. **A** Substrate concentration and biomass accumulation, **B** pH and Xdh activity measurements, and **C** D-xylonate, glycolate, and ethylene glycol concentrations. Alternate shading indicates different cycle times with 36 h interval. At least two independent trials were performed for both strains

2019). Aside from promoters, riboregulators such as the 207-nucleotide pH-responsive RNA element (PRE) that regulates the expression of *alx* gene in *E. coli* were used in a genetic controller and applied in evolutionary engineering experiments (Pham et al. 2017). These studies demonstrate that pH-dependent regulatory systems are useful tools in developing robust synthetic genetic sensors for different applications.

In the present study, a modified transmembrane one-component receptor protein, CadCΔ, was used in developing a pH-responsive sensor for the dynamic control of a pathway intermediate accumulation in *E. coli*. The activation mechanism of CadCΔ is straightforward – the periplasmic domain senses the low pH and promotes overall structural changes which allow the DNA-binding domain to interact and activate the *cadBA* promoter. The simplicity of this genetic circuit makes it a versatile tool for developing a pH sensor coupled to a direct or indirect controller device to prevent the buildup of any compound that causes extracellular pH perturbation. Furthermore, CadCΔ has a good acidic pH sensitivity range that begins at 6.8 and peaks at 5.8 (Slonczewski et al. 1987; Watson et al. 1992), whereas the P_{asr} system requires lower pH values at 4.0 to 4.5 to achieve maximum induction (Šeputienė et al. 2004) while the PRE system is activated at pH 8.0 (Nechooshtan et al. 2009).

Other CadC variants such as the R265C or F165A single mutants have also been demonstrated to be completely pH-dependent (Neely et al. 1994; Tetsch et al. 2008). These mutants were not considered for this study since the said amino acid replacements do not directly block LysP binding; rather, they induce long-range structural and conformational changes to the whole receptor protein that make it less susceptible to LysP interaction (Tetsch et al. 2008). Any perturbation in the cells carrying these single mutants may lead to the loss of their altered tertiary/quaternary structures, especially that they retain a moderate degree of vulnerability in conditions where LysP is overexpressed (Tetsch et al. 2008). Aside from using CadC variants, an alternative pH-dependent genetic sensor may be constructed from an *lysP* knockout strain (Neely et al. 1994). The lack of LysP transporter in this strain can bring about the conversion of the native CadC system in *E. coli* into an exclusively pH-dependent signaling module. However, the CadC receptor protein requires overexpression since the natural expression of CadC only produces up to 3–5 molecules per cell (Jung et al. 2018).

Taken altogether, the results of the study demonstrated for the first time a functional prototype biological circuit that incorporates a pH-responsive regulatory protein in a synthetic genetic controller for D-xylonic acid accumulation (Fig. 3). Unlike any metabolite-responsive transcription factors that interact directly to a specific pathway intermediate (Xu 2018), the CadCΔ protein detects changes in the extracellular pH which is directly influenced by the secreted D-xylonic acid. The response of CadCΔ then cascades into a feedback control signal which inhibits further buildup of the afore-mentioned metabolite. This genetic controller is not compound-specific; hence, it can be customized for other pathways that involve sugar acid degradation such as D-gluconic acid and D-galactonic acid, as well as the DeLey-Doudoroff pathway (Fraenkel and Levisohn 1967; Wong and Yao 1994; Deacon and Cooper 2001). Additionally, this genetic controller eliminates the need to use inorganic acid or base to maintain the culture media pH during fermentation. On the other hand, the main limitation for this pH-responsive genetic circuit may be in its application in metabolic pathways with organic acids as end products

or when the pathway secretes more than one acidic intermediate compound. Under these conditions, the media acidification caused by more than one compound complicates the system. Recruiting other compound-specific biosensors for each target metabolite may be necessary to create discrete modular controls over the accumulation of each compound. However, if the acidic pathway intermediate or by-product is nonessential, blocking its formation through gene knockout may be sufficient, provided that the protein product of the inactivated gene does not play a critical role in maintaining cell viability or fitness. In the case of the Dahms pathway, glycolic acid can contribute to the media acidification; hence, blocking its formation was considered (Fig. S4). However, the deletion of *aldA* in EWEGPH resulted in a poor strain phenotype compared to its parent strain EWXAPH. The same observation was reported in an earlier work that focused on improving the production of ethylene glycol (Liu et al. 2013). This behavior may be attributed to the role of AldA in the oxidative stress response of *E. coli*, wherein it mediates the detoxification (oxidation) of methylglyoxal (Baldoma and Aguilar 1987; Lee and Park 2017).

To summarize, the pH genetic sensor that utilizes a lysine-independent and pH-sensitive CadCΔ receptor protein was effective in providing dynamic regulation of D-xylonic acid accumulation through the detection of extracellular pH fluctuations. It has achieved the goal of minimizing the transient buildup of D-xylonic acid which is the bottleneck of the Dahms pathway or the XOP in general. The genetic sensor also positively affected the formation of ethylene glycol, while the accumulation of glycolic acid was still observed in the model strain. Ultimately, the CadCΔ genetic circuit presented in this study can be considered a great addition to the limited number of DNA chassis in the pH-sensing toolbox available for synthetic biologists.

Funding information This work was supported by Korea Research Fellowship Program through the National Research Foundation of Korea (NRF) funded by the Ministry of Science and ICT (2015H1D3A1062172), by the Ministry of Education (2018R1D1A1B07043993), and by the Korea Institute of Energy Technology Evaluation and Planning (KETEP) funded by the Ministry of Trade, Industry & Energy (MOTIE, No. 20194010201750).

Compliance with ethical standards

Conflict of interest The authors declare that they have no conflict(s) of interest.

Statement of informed consent This article does not contain any studies with human participants performed by any of the authors.

References

Baldoma L, Aguilar J (1987) Involvement of lactaldehyde dehydrogenase in several metabolic pathways of *Escherichia coli* K12. J Biol Chem 262:13991–13996

Bañares AB, Valdehuesa KNG, Ramos KRM, Nisola GM, Lee W-K, Chung W-J (2019) Discovering a novel D-xylonate-responsive promoter: the P_{yjhI}-driven genetic switch towards better 1,2,4-butanetriol production. Appl Microbiol Biotechnol 103:8063–8074. https://doi.org/10.1007/s00253-019-10073-0

Berghäll S, Hilditch S, Penttilä M, Richard P (2007) Identification in the mould *Hypocrea jecorina* of a gene encoding an $NADP^+$: D-xylose dehydrogenase. FEMS Microbiol Lett 277:249–253. https://doi.org/10.1111/j.1574-6968.2007.00969.x

Bradford MM (1976) A rapid and sensitive method for the quantitation of microgram quantities of protein utilizing the principle of protein-dye binding. Anal Biochem 72:248–254. https://doi.org/10.1016/0003-2697(76)90527-3

Cabulong RB, Valdehuesa KNG, Ramos KRM, Nisola GM, Lee W-K, Lee CR, Chung W-J (2017) Enhanced yield of ethylene glycol production from D-xylose by pathway optimization in *Escherichia coli*. Enzym Microb Technol 97:11–20. https://doi.org/10.1016/j.enzmictec.2016.10.020

Cabulong RB, Lee W-K, Bañares AB, Ramos KRM, Nisola GM, Valdehuesa KNG, Chung W-J (2018a) Engineering *Escherichia coli* for glycolic acid production from D-xylose through the Dahms pathway and glyoxylate bypass. Appl Microbiol Biotechnol 102:2179–2189. https://doi.org/10.1007/s00253-018-8744-8

Cabulong RB, Valdehuesa KNG, Bañares AB, Ramos KRM, Nisola GM, Lee W-K, Chung W-J (2018b) Improved cell growth and biosynthesis of glycolic acid by overexpression of membrane-bound pyridine nucleotide transhydrogenase. J Ind Microbiol Biotechnol 46:159–169. https://doi.org/10.1007/s10295-018-2117-2

Choi SY, Park SJ, Kim WJ, Yang JE, Lee H, Shin J, Lee SY (2016) One-step fermentative production of poly(lactate-co-glycolate) from carbohydrates in *Escherichia coli*. Nat Biotechnol 34:435–440. https://doi.org/10.1038/nbt.3485

Chung CT, Niemela SL, Miller RH (1989) One-step preparation of competent *Escherichia coli*: transformation and storage of bacterial cells in the same solution. Proc Natl Acad Sci U S A 86:2172–2175

Dahms AS (1974) 3-deoxy-D-pentulosonic acid aldolase and its role in a new pathway of D-xylose degradation. Biochem Biophys Res Commun 60:1433–1439. https://doi.org/10.1016/0006-291X(74)90358-1

Deacon J, Cooper RA (2001) D-galactonate utilisation by enteric bacteria. FEBS Lett 77:201–205. https://doi.org/10.1016/0014-5793(77)80234-2

Dell CL, Neely MN, Olson ER (1994) Altered pH lysine signalling mutants of cadC, a gene encoding a membrane-bound transcriptional activator of the Escherichia coli cadBA operon. Mol Microbiol 14:7–16. https://doi.org/10.1111/j.1365-2958.1994.tb01262.x

Eichinger A, Haneburger I, Koller C, Jung K, Skerra A (2011) Crystal structure of the sensory domain of *Escherichia coli* CadC, a member of the ToxR-like protein family: crystal structure of CadC. Protein Sci 20:656–669. https://doi.org/10.1002/pro.594

Fraenkel DG, Levisohn SR (1967) Glucose and gluconate metabolism in an *Escherichia coli* mutant lacking phosphoglucose isomerase. J Bacteriol 93:1571–1578

Fritz G, Koller C, Burdack K, Tetsch L, Haneburger I, Jung K, Gerland U (2009) Induction kinetics of a conditional pH stress response system in *Escherichia coli*. J Mol Biol 393:272–286. https://doi.org/10.1016/j.jmb.2009.08.037

Gibson DG, Young L, Chuang R-Y, Venter JC, Hutchison CA, Smith HO (2009) Enzymatic assembly of DNA molecules up to several

hundred kilobases. Nat Methods 6:343–345. https://doi.org/10.1038/nmeth.1318

Gírio FM, Fonseca C, Carvalheiro F, Duarte LC, Marques S, Bogel-Łukasik R (2010) Hemicelluloses for fuel ethanol: a review. Bioresour Technol 101:4775–4800. https://doi.org/10.1016/j.biortech.2010.01.088

Green MR, Sambrook J (2012) Molecular cloning: a laboratory manual, 4 edn. Cold Spring Harbor Laboratory Press, New York

Haas BL, Matson JS, Dirita VJ, Biteen JS (2015) Single-molecule tracking in live Vibrio cholerae reveals that ToxR recruits the membrane-bound virulence regulator TcpP to the toxT promoter. Mol Microbiol 96:4–13. https://doi.org/10.1111/mmi.12834

Haneburger I, Eichinger A, Skerra A, Jung K (2011) New insights into the signaling mechanism of the pH-responsive, membrane-integrated transcriptional activator CadC of *Escherichia coli*. J Biol Chem 286:10 681–10 689. https://doi.org/10.1074/jbc.M110.196923

Haneburger I, Fritz G, Jurkschat N, Tetsch L, Eichinger A, Skerra A, Gerland U, Jung K (2012) Deactivation of the *E. coli* pH stress sensor CadC by cadaverine. J Mol Biol 424:15–27. https://doi.org/10.1016/j.jmb.2012.08.023

Hoynes-OConnor A, Shopera T, Hinman K, Creamer JP, Moon TS (2017) Enabling complex genetic circuits to respond to extrinsic environmental signals. Biotechnol Bioeng 114:1626–1631. https://doi.org/10.1002/bit.26279

Jung K, Fabiani F, Hoyer E, Lassak J (2018) Bacterial transmembrane signalling systems and their engineering for biosensing. Open Biol 8:180023. https://doi.org/10.1098/rsob.180023

Lee C, Park C (2017) Bacterial responses to glyoxal and methylglyoxal: reactive electrophilic species. Int J Mol Sci 18:169. https://doi.org/10.3390/ijms18010169

Lindner E, White SH (2014) Topology, dimerization and stability of the single-span membrane protein CadC. J Mol Biol 426:2942–2957. https://doi.org/10.1016/j.jmb.2014.06.006

Liu H, Lu T (2015) Autonomous production of 1,4-butanediol via a *de novo* biosynthesis pathway in engineered *Escherichia coli*. Metab Eng 29:135–141. https://doi.org/10.1016/j.ymben.2015.03.009

Liu H, Valdehuesa KNG, Nisola GM, Ramos KRM, Chung W-J (2012) High yield production of D-xylonic acid from D-xylose using engineered *Escherichia coli*. Bioresour Technol 115:244–248. https://doi.org/10.1016/j.biortech.2011.08.065

Liu H, Ramos KRM, Valdehuesa KNG, Nisola GM, Lee W-K, Chung W-J (2013) Biosynthesis of ethylene glycol in *Escherichia coli*. Appl Microbiol Biotechnol 97:3409–3417. https://doi.org/10.1007/s00253-012-4618-7

Meijnen J-P, de Winde JH, Ruijssenaars HJ (2009) Establishment of oxidative D-xylose metabolism in *Pseudomonas putida* S12. Appl Environ Microbiol 75:2784–2791. https://doi.org/10.1128/AEM.02713-08

Nechooshtan G, Elgrably-Weiss M, Sheaffer A, Westhof E, Altuvia S (2009) A pH-responsive riboregulator. Genes Dev 23:2650–2662. https://doi.org/10.1101/gad.552209

Neely MN, Olson ER (1996) Kinetics of expression of the *Escherichia coli cad* operon as a function of pH and lysine. J Bacteriol 178:5522–5528

Neely MN, Dell CL, Olson ER (1994) Roles of LysP and CadC in mediating the lysine requirement for acid induction of the *Escherichia coli cad* operon. J Bacteriol 176:3278–3285. https://doi.org/10.1128/jb.176.11.3278-3285.1994

Pédelacq J-D, Cabantous S, Tran T, Terwilliger TC, Waldo GS (2006) Engineering and characterization of a superfolder green fluorescent protein. Nat Biotechnol 24:79–88. https://doi.org/10.1038/nbt1172

Pham HL, Wong A, Chua N, Teo WS, Yew WS, Chang MW (2017) Engineering a riboswitch-based genetic platform for the self-directed evolution of acid-tolerant phenotypes. Nat Commun 8:411. https://doi.org/10.1038/s41467-017-00511-w

Radek A, Krumbach K, Gätgens J, Wendisch VF, Wiechert W, Bott M, Noack S, Marienhagen J (2014) Engineering of *Corynebacterium glutamicum* for minimized carbon loss during utilization of D-xylose containing substrates. J Biotechnol 192(Pt a):156–160. https://doi.org/10.1016/j.jbiotec.2014.09.026

Rajkumar AS, Liu G, Bergenholm D, Arsovska D, Kristensen M, Nielsen J, Jensen MK, Keasling JD (2016) Engineering of synthetic, stress-responsive yeast promoters. Nucleic Acids Res 44:e136. https://doi.org/10.1093/nar/gkw553

Roberts TM, Rudolf F, Meyer A, Pellaux R, Whitehead E, Panke S, Held M (2016) Identification and characterisation of a pH-stable GFP. Sci Rep 6:28166. https://doi.org/10.1038/srep28166

Salusjärvi L, Toivari M, Vehkomäki M-L, Koivistoinen O, Mojzita D, Niemelä K, Penttilä M, Ruohonen L (2017) Production of ethylene glycol or glycolic acid from D-xylose in *Saccharomyces cerevisiae*. Appl Microbiol Biotechnol 14:127–113. https://doi.org/10.1007/s00253-017-8547-3

Šeputienė V, Sužiedėlis K, Normark S, Melefors Ö, Sužiedėlienė E (2004) Transcriptional analysis of the acid-inducible *asr* gene in enterobacteria. Res Microbiol 155:535–542. https://doi.org/10.1016/j.resmic.2004.03.010

Slonczewski JL, Gonzalez TN, Bartholomew FM, Holt NJ (1987) Mu d-directed *lacZ* fusions regulated by low pH in *Escherichia coli*. J Bacteriol 169:3001–3006. https://doi.org/10.1128/jb.169.7.3001-3006.1987

Stirling F, Naydich A, Bramante J, Barocio R, Certo M, Wellington H, Redfield E, O'Keefe S, Gao S, Cusolito A, Way J, Silver P (2019) Synthetic cassettes for pH-mediated sensing, counting and containment. bioRxiv 740902. doi: https://doi.org/10.1101/740902

Sun L, Yang F, Sun H, Zhu T, Li X, Li Y, Xu Z, Zhang Y (2016) Synthetic pathway optimization for improved 1,2,4-butanetriol production. J Ind Microbiol Biotechnol 43:67–78. https://doi.org/10.1007/s10295-015-1693-7

Takayama M, Ohyama T, Igarashi K, Kobayashi H (1994) Escherichia coli cad operon functions as a supplier of carbon dioxide. Mol Microbiol 11:913–918. https://doi.org/10.1111/j.1365-2958.1994.tb00370.x

Tetsch L, Koller C, Haneburger I, Jung K (2008) The membrane-integrated transcriptional activator CadC of *Escherichia coli* senses lysine indirectly via the interaction with the lysine permease LysP. Mol Microbiol 67:570–583. https://doi.org/10.1111/j.1365-2958.2007.06070.x

Valdehuesa KNG, Liu H, Ramos KRM, Park SJ, Nisola GM, Lee W-K, Chung W-J (2014) Direct bioconversion of D-xylose to 1,2,4-butanetriol in an engineered *Escherichia coli*. Process Biochem 49:25–32. https://doi.org/10.1016/j.procbio.2013.10.002

Valdehuesa KNG, Lee W-K, Ramos KRM, Cabulong RB, Choi J, Liu H, Nisola GM, Chung W-J (2015) Identification of aldehyde reductase catalyzing the terminal step for conversion of xylose to butanetriol in engineered *Escherichia coli*. Bioprocess Biosyst Eng 38:1761–1772. https://doi.org/10.1007/s00449-015-1417-4

Valdehuesa KNG, Ramos KRM, Nisola GM, Bañares AB, Cabulong RB, Lee W-K, Liu H, Chung W-J (2018) Everyone loves an underdog: metabolic engineering of the xylose oxidative pathway in recombinant microorganisms. Appl Microbiol Biotechnol 102:7703–7716. https://doi.org/10.1007/s00253-018-9186-z

Wang C, Wei D, Zhang Z, Wang D, Shi J, Kim CH, Jiang B, Han Z, Hao J (2016) Production of xylonic acid by *Klebsiella pneumoniae*. Appl Microbiol Biotechnol 100:10055–10063. https://doi.org/10.1007/s00253-016-7825-9

Wang X, Xu N, Hu S, Yang J, Gao Q, Xu S, Chen K, Ouyang P (2018) D-1,2,4-Butanetriol production from renewable biomass with optimization of synthetic pathway in engineered *Escherichia coli*. Bioresour Technol 250:406–412. https://doi.org/10.1016/j.biortech.2017.11.062

Watson N, Dunyak DS, Rosey EL, Slonczewski JL, Olson ER (1992) Identification of elements involved in transcriptional regulation of the *Escherichia coli cad* operon by external pH. J Bacteriol 174: 530–540

Weimberg R (1961) Pentose oxidation by *Pseudomonas fragi*. J Biol Chem 236:629–635

Wong TY, Yao XT (1994) The DeLey-Doudoroff pathway of galactose metabolism in *Azotobacter vinelandii*. Appl Environ Microbiol 60: 2065–2068

Xu P (2018) Production of chemicals using dynamic control of metabolic fluxes. Curr Opin Biotechnol 53:12–19. https://doi.org/10.1016/j.copbio.2017.10.009

Xu P, Vansiri A, Bhan N, Koffas MAG (2012) ePathBrick: a synthetic biology platform for engineering metabolic pathways in *E. coli*. ACS Synth Biol 1:256–266. https://doi.org/10.1021/sb300016b